

Effects of annealing and strain on $\text{La}_{1-x}\text{Ca}_x\text{MnO}_3$ thin films : a new phase diagram in the ferromagnetic region

W. Prellier, M. Rajeswari, T. Venkatesan and R.L. Greene

Center for Superconductivity Research, Department of Physics, University of

Maryland, College Park, MD 20742, USA

Oriented, single phase thin films of $\text{La}_{1-x}\text{Ca}_x\text{MnO}_3$ have been deposited onto (100)-oriented LaAlO_3 ($0.1 < x < 0.5$) substrates using the Pulsed Laser Deposition technique. While for some compositions the physical properties (transport and magnetization) of the as-grown films are higher than the bulk values, for other calcium contents the optimized properties are obtained only after annealing under oxygen. These data can be partly explained by changes in oxygen content, resulting in cationic vacancies and thus self-doping effects - accompanying structural changes, may be the cause of properties beyond the phase diagram. We propose a new phase diagram for $(\text{La}_{1-x}\text{Ca}_x)_{1-y}\square_y\text{MnO}_3$ ($0.1 < x < 0.5$) thin films.

There has been a lot of recent interest in the properties of manganites such as $\text{RE}_{1-x}\text{A}_x\text{MnO}_3$ (RE is a rare earth such as La, Pr, Nd and A is an alkaline earth such as Ca, Ba or Sr) in particular due to a spectacular decrease of electrical resistance under a magnetic field [1], the so-called colossal magnetoresistance (CMR) [2]. Due to the long history of work on these compounds, most of the studies have been performed on bulk ceramic samples. For example, it was demonstrated that chemical substitution on the trivalent ion sites can have an effect similar to annealing (i.e. changing the $\text{Mn}^{3+}/\text{Mn}^{4+}$ ratio). Also, the determination of the "phase diagram" upon alkaline earth doping has been achieved essentially on ceramics samples [3,4].

The basic phenomena of the CMR effect seems to be the same in bulk and thin film samples. However, due to the strain effect of the substrate or oxygen deficiency, it is often difficult to reach in a thin film the same properties as the bulk [5–7]. But surprisingly, it has been shown recently that an anomalously high metal-insulator transition (T_{MI}) occurs in thin films of nominal composition $\text{La}_{0.8}\text{Ca}_{0.2}\text{MnO}_3$ [8] (T_{MI} is near room temperature, 100 K higher than the bulk value [3]). For these reasons, we decided to investigate the effect of doping and annealing in thin films deposited on LaAlO_3 substrates for the solid solution $\text{La}_{1-x}\text{Ca}_x\text{MnO}_3$ ($0 < x < 0.5$). We have compared the properties of as-grown films and post-annealed ones under oxygen or argon flux. We have obtained the phase diagram as a function of temperature (T) and x, for both as-grown and oxygen annealed films, which is significantly different from the bulk one [3,4]. These data are compared and discussed with bulk ceramics.

Thin films of $\text{La}_{1-x}\text{Ca}_x\text{MnO}_3$ (LCMO) were grown using the Pulsed Laser Deposition (PLD) technique. The targets used had a nominal composition of $\text{La}_{1-x}\text{Ca}_x\text{MnO}_3$ ($x=0.1, 0.15, 0.2, 0.25, 0.33, 0.4$ and 0.5). Most of the films were synthesized on $[100]$ LaAlO_3 substrates, which has a pseudocubic crystallographic structure with $a=3.79$ Å. The laser energy density on the target was about 1.5 J/cm^2 and the deposition rate was 10 Hz. The substrates were kept at a constant temperature of 820°C during the deposition which was carried out at a pressure of 400 mTorr of oxygen. After deposition, the samples were slowly

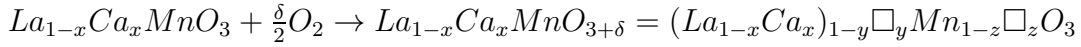
cooled to room temperature at a pressure of 400 Torr of oxygen. All films had a thickness around 1500 Å. Further details of the target preparation and the deposition procedure are given elsewhere [5]. The annealing was done under flowing oxygen or argon at 800 °C for 10 h. The heating and the cooling were done at 10 °C/min. Note that the temperature of annealing is below the synthesis temperature in order to keep the same structure as the one obtained during the laser ablation process. The structural study was carried out by X-ray diffraction (XRD) using a Rigaku diffractometer with the usual $\Theta - 2\Theta$ scan. DC resistivity (ρ) was measured by a standard four-probe method and the magnetization (M) was obtained using a Quantum Design MPMS SQUID magnetometer.

The X-ray diffraction data indicate that all the films are single phase since only two sharp diffraction peaks at around $2\Theta \approx 23^\circ$ and 46° appear (see inset of Fig.1 for $x=0.25$). They correspond to an out-of-plane parameter proportional to the ideal parameter of cubic perovskite (≈ 3.9 Å). It is not possible on the basis of this pattern to tell if the film is [110] or [001]-oriented, however, this does not matter for the conclusions of this paper. Fig.1 shows simultaneously the evolution of the out-of-plane parameter as a function of x for an as-grown and an oxygen annealed film. We also show some values given by Huang et al. [9] on ceramic samples. Two features can be seen from this graph. First, a small decrease of the out-of-plane parameter with increasing calcium content is found and this is consistent with the formation of mixed valence $\text{Mn}^{3+}/\text{Mn}^{4+}$ [10]. Second, for a given composition, a decrease of this parameter is found after annealing under oxygen and this change is more pronounced for lower doping of calcium (for example at $x=0.15$, we have 3.93 Å for the as-grown film and 3.87 Å for the annealed film).

Fig.2 shows the DC magnetization taken under a magnetic field of 2000 Oe for the as-grown and annealed film of $x=0.25$. The Curie temperature (T_c) is increased from about 240 K to 270 K after oxygen annealing. At the same time, the metal-insulator transition T_{MI} (see inset of Fig.2) increases from about 250 K to 281 K. The difference between T_c and T_{MI} is most likely a particle size effect [11] which is consistent with our observations that the full width at half maximum of the diffraction peak decreases upon annealing (from

0.2° to 0.1° after annealing). The increase of the transition temperature under annealing is not surprising since it is well known that this treatment can often improve the physical properties of manganites and also other oxides [12]. However, it is surprising that both T_{MI} and T_c are much higher than the bulk values previously reported by Shriver et al. [3].

The saturation magnetization value, obtained with a magnetic field of 2 T, is $3.75 \mu_B$ for the as-grown film (the expected theoretical value), but is $3.59 \mu_B$ after oxygen annealing. This change can be interpreted as an increase of the Mn^{4+}/Mn^{3+} ratio after annealing. An increase of Mn^{4+} would explain why T_c and T_{MI} also increase, at least according to the bulk phase diagram [3,4] (see Fig.5). This suggests that under oxygen annealing the oxygen content in the film is increasing and we expect :



(where \square represents cations vacancies and δ this excess of oxygen)

Thus, excess oxygen leads to an equal number of vacancies at both of the cation sites [13] and therefore to an increase of the Mn^{4+} content. To check if these changes are related to oxygen incorporation or thermally effects, we have annealed the as-grown film ($La_{0.75}Ca_{0.25}MnO_3$ on $LaAlO_3$) under argon and oxygen at the same temperature. The resistivity of both samples is presented in Fig.3. The effect of argon is negligible for the T_{MI} and the out-of plane parameter remains unchanged ($\approx 3.86 \text{ \AA}$). Also, the temperature coefficient of resistance ($1/RdR/dT$) is nearly the same. Thus, the effect of annealing is from oxygen incorporation and not the temperature.

The shift towards the Mn^{4+} rich region of the phase diagram under oxygen annealing is more pronounced for a low doping of calcium as already reported for bulk samples [14]. As an example, we show in Fig.4 the effect of oxygen annealing for a film with composition $La_{0.9}Ca_{0.1}MnO_3$ deposited on $LaAlO_3$. The as-grown film is an insulator, as expected from the bulk phase diagram, but after oxygen annealing displays a metal-insulator transition at 170 K. Again, this is a result of increased Mn^{4+} and is perfectly consistent with the bulk phase diagram since $x=0.1$, is already close to the boundary between the insulator and metallic regions ($x \approx 0.175$). In addition, under oxygen annealing the change of the out-of-

plane parameter is very strong, consistent with the formation of cation vacancies at the La and Mn sites [15].

We summarize these data in Fig.5 with a plot of the film phase diagram for the composition range $x=0.1$ to $x=0.5$. There is clearly a difference from the bulk phase diagram (dashed line in Fig.5). Some of this difference can be explained by 'self-doping' effects related to increase in Mn^{4+} due to cation vacancies. But this is not sufficient to explain why for the $x=0.2$ composition, T_{MI} is 30 K higher than the highest T_{MI} found in any bulk phase (i.e. $T_{MI} \approx 260$ K for $x=0.33$). It is possible that the presence of cationic vacancies also result in structural changes which be more easily accommodated in thin film form (i.e. strain-induced by the substrate). For instance, if the cationic vacancies would lead to an internal pressure, i.e. decreased with cell volume, we may expect the T_{MI} and T_c to be higher as for hydrostatic pressure effects in bulk [16,17]. We are currently undertaken detailed structural studies.

In summary, we have investigated the structural, magnetic and transport properties of a series of $\text{La}_{1-x}\text{Ca}_x\text{MnO}_3$ deposited on LaAlO_3 in order to better understand the effect of composition on the properties of thin films. We found that the thin film phase diagram is somewhat different than that of the bulk. Oxygen annealing leads to an enhancement of T_{MI} and T_c . We explain this as resulting from two related contributions : the strains induced by the substrate and the change in oxygen stoichiometry (leading to cation vacancies) due the annealing.

Acknowledgments

Partial support of NSF-MRSEC at University of Maryland is acknowledged (DMR #96-32521). We thank Z. Li for the preparation of targets, M. Lewis for transport measurements and R.C. Srivastava for XRD measurements.. We acknowledge A. Biswas and P.A. Salvador for helpful discussions.

-
- [1] R. von Helmolt, J. Wecker, B. Holzapfel, L. Schultz and K. Samwer, Phys. Rev. Lett. 71, 2331 (1993)
- [2] S. Jin, T.H. Tiefel, M. McCormack, R.A. Fastnacht, R. Ramesh and L.H. Chen, Science 264, (1994) 413.
- [3] P. Schiffer, A.P. Ramirez, W. Bao and S.W. Cheong, Phys. Rev. Lett. 75, 3336 (1995).
- [4] S.W. Cheong, C.M. Lopez and H. Y. Hwang (private communication).
- [5] H.L. Ju, C. Kwon, Q. Li, R.L. Greene and T. Venkatesan, App. Phys. Lett. 65, 2104 (1994).
- [6] G.C. Xiong, Q. Li, H.L. Ju, S.N. Nao, L. Senapati, X.X. Xi, R.L. Greene and T. Venkatesan, App. Phys. Lett. 66, 1427 (1995).
- [7] W. Prellier, A. Biswas, M. Rajeswari, T. Venkatesan and R.L. Greene (unpublished).
- [8] R. Shreekala, M. Rajeswari, R.C. Srivatava, K. Ghosh, A. Goyal, V.V. Srinivasu, S.E. Ioffland, S.M. Bhagat, M. Downes, R.P. Sharma, S.B. Ogale, R.L. Greene, R. Ramesh, T. Venkatesan, R.A. Rao and C.B. Eom, Appl. Phys Lett. 74, 1886 (1999).
- [9] Q. Huang, A. Santoro, J.W. Lynn, R.W. Erwin, J.A. Borchers, J.L. Peng, K. Ghosh and R.L. Greene, Phys. Rev. B 58, 2684 (1998).
- [10] E.O. Wollan and W.C. Koehler, Phys. Rev. 100, 545 (1955).
- [11] R. Mahesh, R. Mahendiran, A.K. Raychaudhuri and C.N.R. Rao, App. Phys. Lett. 68, 2291 (1996).
- [12] W. Chang, J.S. Horwitz, A.C. Carter, J.N. Pond, S.W. Kirchoefer, C.M. Gilmore and D.B. Chrisey, App. Phys. Lett. 74, 1033 (1999).
- [13] B. Dabrowski, P.W. Klamut, Z. Bukowski, R. Dybziński and J.E. Siewenie, Jour. Sol. State.

Chem. 144, 461 (1999).

- [14] Q. Huang, A. Santoro, J.W. Lunn, R.W. Erwin, J.A. Borchers, J.L. Peng and R.L. Greene, Phys. Rev. B 55, 14987 (1997).
- [15] A. Gupta, T.R. McGuire, P.R. Duncombe, M. Rupp, J.Z. Sun, W.J. Gallagher and G. Xiao, App. Phys. Lett. 67, 3494 (1995).
- [16] J.J. Neumeier, M.F. Hundley, J.D. Thompson and R.H. Heffner, Phys. Rev. B 52, 7006 (1995).
- [17] H.Y. Hwang, T.T.M. Palstra, S-W. Cheong and B. Batlogg, Phys. Rev. B 52, 15046 (1995).

Figure captions

Fig.1 : Evolution of the out-of-plane parameter vs x in thin films of $\text{La}_{1-x}\text{Ca}_x\text{MnO}_3$ deposited on LaAlO_3 substrates. Solid and open squares correspond respectively to the as-grown and annealed films. We also show the bulk lattice parameters from Ref. [9] (open triangles : c axis, solid triangles : a, b axes). Lines are only a guide for the eyes. The inset shows the diffractogram of as-grown $\text{La}_{0.75}\text{Ca}_{0.25}\text{MnO}_3$ on LaAlO_3 .

Fig.2 : DC magnetization vs temperature for a $\text{La}_{0.75}\text{Ca}_{0.25}\text{MnO}_3$ thin film on LaAlO_3 taken with a magnetic field of 2000 Oe. Squares and circles correspond respectively to the as-grown and the oxygen annealed films. The inset shows $\rho(T)$ for the same films.

Fig.3 : $\rho(T)$ after different annealing treatment (as-grown, oxygen and argon annealing) for $\text{La}_{0.75}\text{Ca}_{0.25}\text{MnO}_3$ on LaAlO_3 .

Fig.4 : $\rho(T)$ for a $\text{La}_{0.9}\text{Ca}_{0.1}\text{MnO}_3$ film on LaAlO_3 . Comparison between an as-grown and oxygen annealed film.

Fig.5 : Phase diagram for $\text{La}_{1-x}\text{Ca}_x\text{MnO}_3$. T_c and T_{MI} are taken from the inflection point in $M(T)$ and $\rho(T)$. Dashed line indicates the data from Ref. [3-4]. Gray dashed lines separate the different regions. Solid lines are only a guide for the eyes.

